

Received: 14 January 2019 / Accepted: 15 April 2019 / Published online: 29 June 2019

*chatter, ball-screw,
feed-drive*

Jan GRAU^{1*}
Matej SULITKA¹
Pavel SOUCEK¹

INFLUENCE OF LINEAR FEED DRIVE CONTROLLER SETTING IN CNC TURNING LATHE ON THE STABILITY OF MACHINING

The paper deals with the influence of linear feed drive controller setting of a CNC turning lathe on the stability of machining. A coupled simulation model of feed drive control and ball screw drive mechanics with a transmission belt was created and validated by the feed drive diagnostic measurements. The influence of drive control on the overall dynamic compliance at the TCP and the limits of stable depth of cut was examined. Impact of the feed drive actual kinematics configuration on the stability limits was studied as well.

1. INTRODUCTION

Producing a workpiece in a shorter time, with higher accuracy, quality and at a lower cost is a permanent goal of the optimization of machining operations. This represents a complex task, ranging from the selection of workpiece clamping, fixturing system, to the selection of machining strategies, cutting tools, process conditions and last, but not least also the setting of the machine tool CNC control parameters and parameters of the feed drive controllers.

One of the main limiting factors in achieving higher productivity and quality of machining is the issue of chatter vibration. Elevated vibration causes on one hand higher torque and load of the spindle and cutting tools, resulting in shortening their lifetime, on the other hand surfaces with deteriorated quality are produced, which may even lead to production of completely irreparable workpiece surface. A survey of the techniques and procedures improving the machining productivity, including the cutting process stability in production machines can be found in e.g. [1] summarized by Quintana and Ciurana. There are many different types of vibrations entering the cutting process, however already in 1907 Taylor explains in [2] that it is chatter causing the most issues during machining. Deeper view in the chatter identification and recognition is done by Tlustý and Poláček in [3] and independently by Tobias and Fishwick in [4].

¹ CTU – Czech Technical University in Prague, Faculty of Mechanical Engineering, Department of Production Machines and Equipment, Prague, Czech Republic

* E-mail: jan.grau@rcmt.cvut.cz

<https://doi.org/10.5604/01.3001.0013.2221>

Many approaches have been developed to describe machining stability, for example by Merritt in [5]. One of the most generally applied ones is presented by Altintas in [6] where the theory of creating “stability lobe diagram” is introduced based on the frequency response functions of the real machine or the mathematical model. General insight to the current machining stability and chatter issues presents Stone in [7].

Chatter avoidance represents one of the main topics in research and industrial applications. Increased level of machining stability may be achieved by increasing the dynamic stiffness of the machine – cutting tool – workpiece system. Several solutions may be applied:

- Optimized machine tool structural design for increased dynamic stiffness;
- Implementation of passive and active dampers;
- Optimized setting of the feed drive control.

The most effective approach to enhancing the machine tool dynamic stiffness is represented by structural optimization. The Integrated approach to machine tool structural optimization is described by e.g. Kolar in [8] or [9]. Optimization considering the use of hybrid material combinations is presented by Möhring in [10] where mineral cast filling is used for achieving higher dynamic stiffness and consequently higher machining performance. The influence of three-jaw and four-jaw chuck on process stability and generating of so-called parametric vibration inspects Ito in [11].

An increase of dynamic stiffness can be achieved by applying external passive or active dampers as well. The use of external active dampers is presented by Cowley in [12], where the application of accelerometers allows monitoring the input vibrations, according to which the damper is controlled. Adaptive adjustment of the system control by processing the signals from sensors placed close to the cutting operation is presented by Bleicher in [13]. Survey of techniques of vibration suppression is summarized by Munoa in [14] or Novotny in [15]. Using inertial actuators dampers for chatter suppression is presented by Guillerna in [16]. Except for the machine tool mechanical structure, feed drive control represents another source of dynamic compliance and hence the reduced level of machining stability. Lehotzky clarifies in [17] the use of a simple PD controller and its impact on machining stability. Direct feed drive model focusing on the investigation of the control parameters setup is presented by Beudaert in [18]. Two mass model of machine tool structure and simple approximation of cutting force is used. A possible increase of the stable limit of cut by modified feed drive controller parameters is demonstrated.

In this paper, the impact of a ball screw drive controller parameters setting on machining stability is investigated. A detailed model of the linear feed drive mechanics of a lathe is developed and coupled together with experimentally identified directional compliance of the spindle. It is established that the spindle compliance represents an essential part of the entire system dynamic compliance.

2. MODEL

The closest approach to the real situation is in this paper based on creating coupled model of the feed drive, state space model of the motion X_2 axis structure shown in Fig. 1, to

which is attached dynamic compliance of the spindle. Orthogonal grooving operation is taken into an account. This model is shown in scheme in Fig. 2.

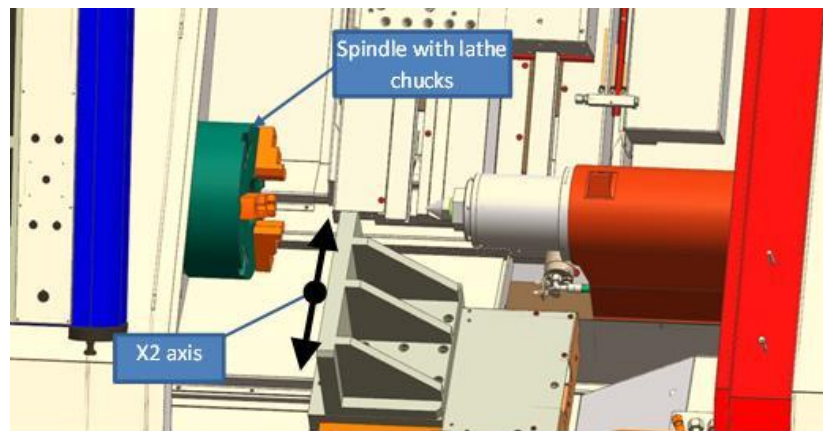


Fig. 1. Middle size lathe workspace

The feed drive part of the mathematical model is based on the widely used cascade regulation. All the drive control parameters are copied out directly from the machine control system Sinumerik.

In the regulation part, the current loop is approximated by the 1st order transfer function measured in the machine control system. The width of the passband for the simulation purposes is set to 547 Hz based on the measured Bode diagram of the lathe current control loop. The velocity control loop is closed by the velocity feedback signal obtained from the rotary motor. Velocity loop is controlled by the proportional P controller with the K_v gain. The outer control loop, the position loop is closed with the position feedback signal from the ruler placed on the $X2$ axis, this is known as direct feedback. The position feedback loop is controlled by the proportional-integral PI controller with the K_p gain and T_n time constant.

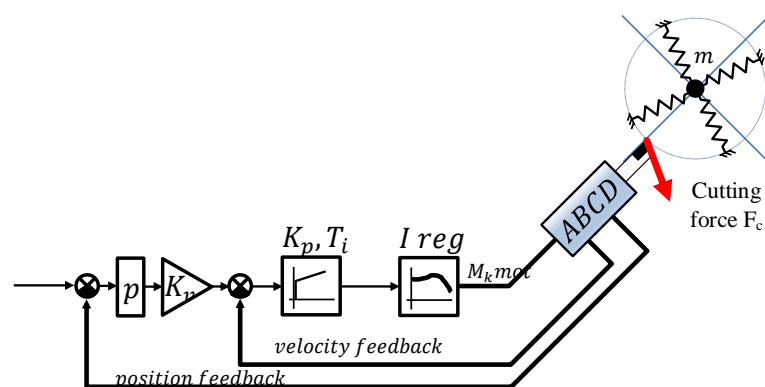


Fig. 2. Model of the system

The mechanic of the $X2$ axis consists of the Siemens motor and pulley connected to the second pulley by a belt. The linear movement of the investigated axis is provided by the ball screw with a double set of axial-radial bearing only on one side as shown in Fig. 3.

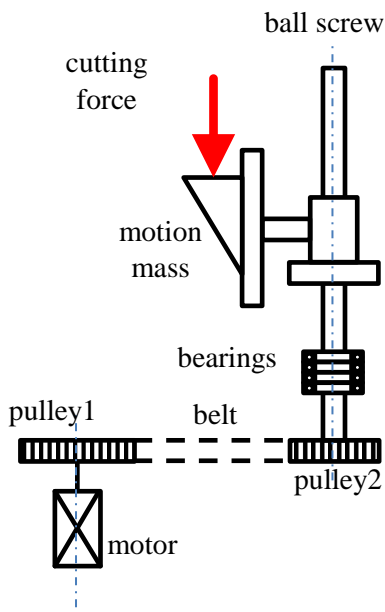


Fig. 3. Axis X2 mechanic structure

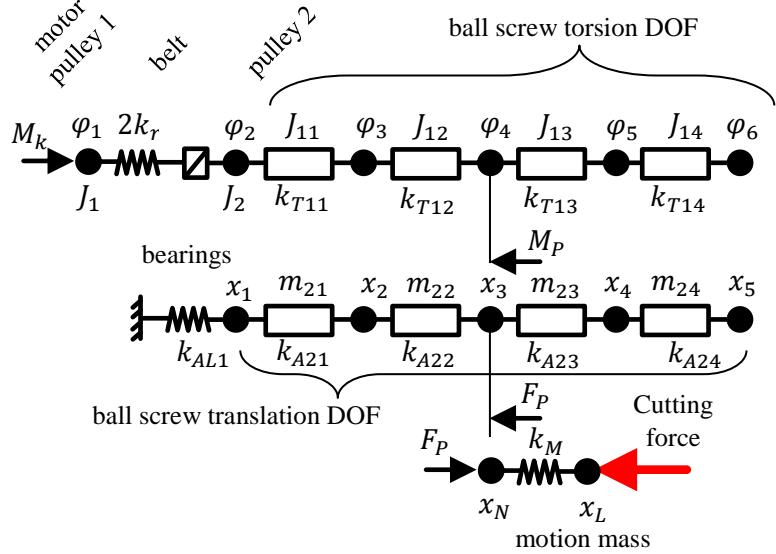


Fig. 4. Axis X2 mechanics discretization

Due to the small stroke of the X2 axis, the discretization pattern shown in Fig. 4 is accepted (with M indicating torques, F for forces, m for masses, J for a moment of inertia, x and φ for positions and k for stiffness). Drawing-up equation of motion following [19] the ABCD state-space model was composed. The approximation of the X2 axis feed drive is done by simplification of the whole moving group and creating coupled ABCD model based on the axis components parameters.

Lathe spindle model is represented by one mass moving in 2D space with two perpendicularly situated springs (see in Fig. 2).

2.1. MODEL VERIFICATION

All three systems described above are created as the closest approach to the real configuration in the X2 axis in the middle size lathe. The regulation parameters are copied directly from the Sinumerik control panel. For the set of drive control regulation constants $K_v = 3$ (m/min)/mm, $K_p = 2.66$ Nms/rad, $T_n = 10$ ms regulation parameters the Bode plot for velocity loop was obtained, the measured characteristic is shown in the Fig. 5 as the blue line and. The red line represents used mathematical approximation. The system frequency corresponding passband is marked as well

For the X2 mechanic configuration, all the mechanic components properties are obtained directly from the machine tool producer and its list value is slightly adjusted based on the transfer function measurement in Fig. 5 Sinumerik controlling system allows the user to get the transfer function of the input velocity to its output value directly from Sinumerik control system with the use of the Siemens Startup Tool software, such an FRF function can be seen in the Fig. 5.

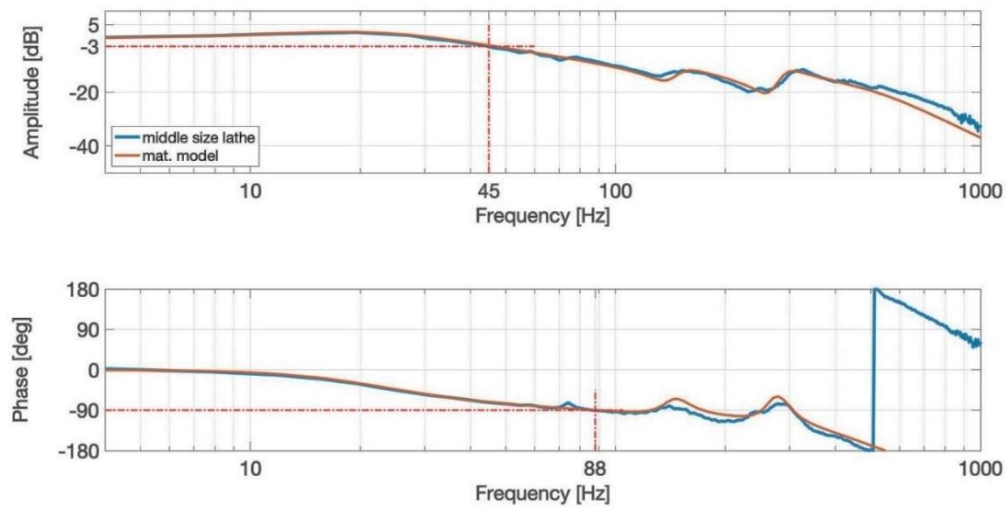


Fig. 5. Bode plot velocity loop

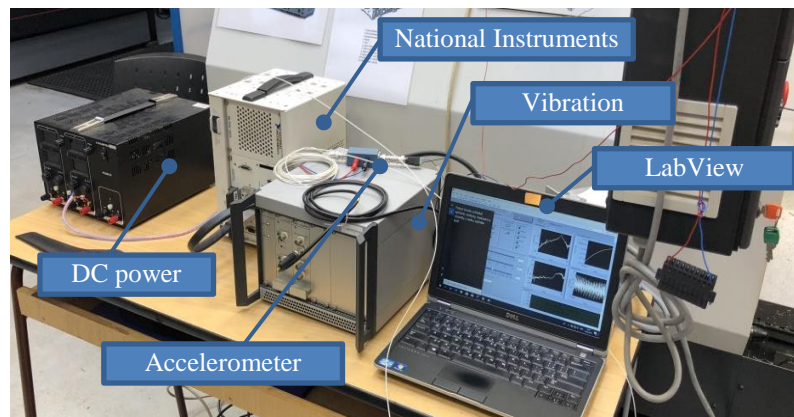


Fig. 6. Measuring equipment

Last verification part takes into account the lathe spindle. For the stability simulation purposes, the vibration – diagnostic was used. The set-up of the experiment can be seen in Fig. 6. Vibration source is held by the lathe chucks, wherein the inner part of vibration source and lathe spindle the accelerometer is installed. For the signal analysis, the LabView software was used. The exciting signal was a sine wave with the maximal force of $F_{\text{vib}} = 31.5 \text{ N}$. Frequency response was measured from the top of the spindle for $\gamma = 0$ (the exact set-up shown in Fig. 7) up to $\gamma = 180 \text{ deg.}$, with the step of 10 deg. adjusted by the machine tool control system. Exciting frequency was applied with the step of 0.5 Hz starting at 20 Hz ending at 400 Hz .

For every single measuring minimum of 20 amplitudes was used and the pause of 0.5 s is applied between each measuring process. Set of all the measurements is shown in Fig. 8. There are two appreciable natural frequencies f , the first one at about 155 Hz and the second one at about 280 Hz . Measured acceleration a is in m/s^2 and the acting force F has the value of approx. 31.5 N . To obtain the position values the double integration takes place accordingly to the equation (1) for every γ from 0 to 180 deg. (defined in Fig. 7).

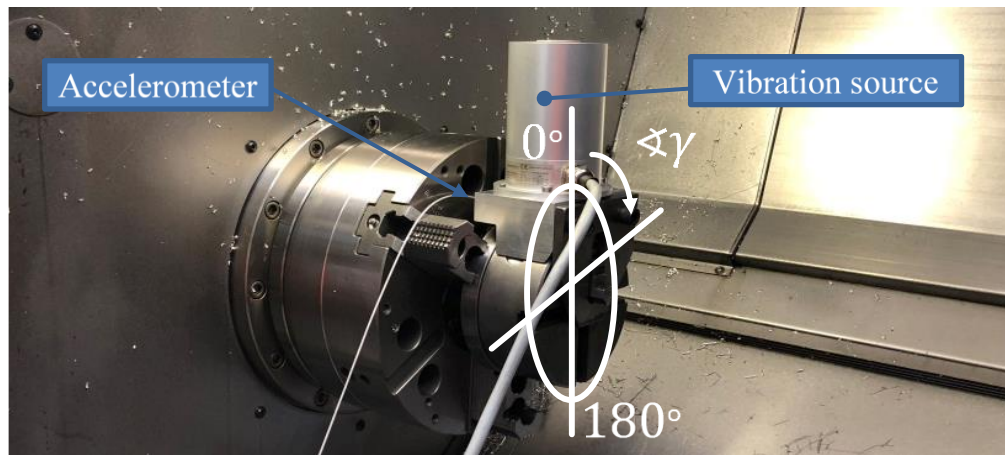


Fig. 7. Vibro-diagnostic configuration

$$G'(\text{spindle}) = \frac{x}{F} = \frac{a}{(2 \cdot \pi \cdot f)^2} \tag{1}$$

When solving the exact value of dynamic compliance for every angle, the polar-chart in Fig. 9 is created. The whole chart in Fig. 9 is composed of measured transfer functions in the range from 0 to 180 deg. The second half of the chart (from 180 to 360 deg.) is generated by overturning of the original values.

Based on the machine structure where the X2 axis interacts with the lathe spindle in the angle of 45 deg. (see the Cutting Force orientation in Fig. 9 and the lathe structure in Fig. 2 or axis X2 orientation in Fig. 3) the designated transfer function is extracted from the polar chart. Full stability model simulation requires identification of the 45 deg. Directional FRF, therefore only 40 deg. and 50 deg. were used for the mathematical model design. Fig. 10 shows in red line the identified transfer function used for the MATLAB – Simulink stability simulations.

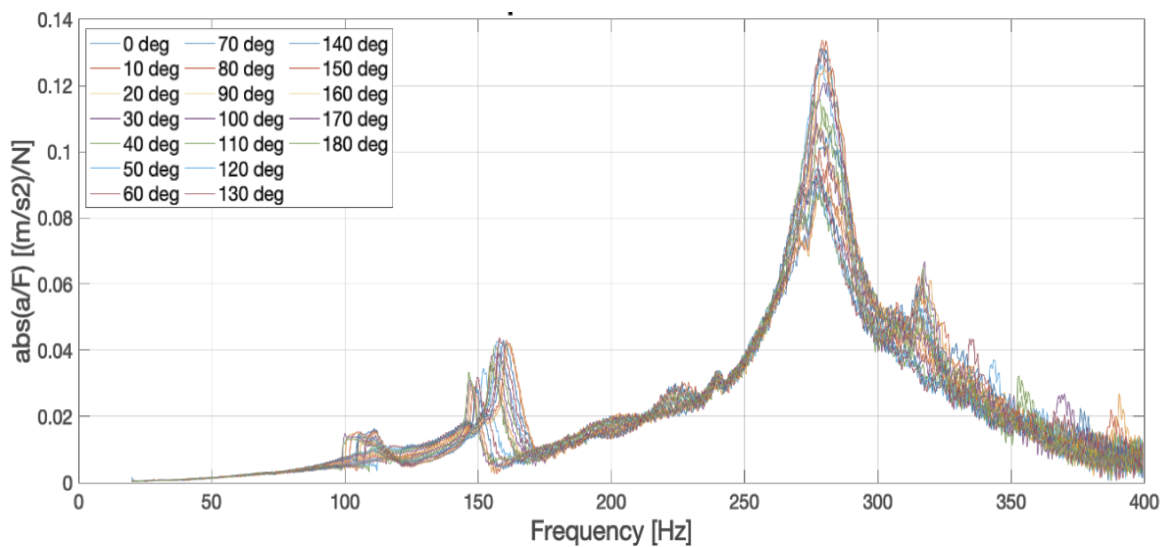


Fig. 8. Lathe spindle transfer function

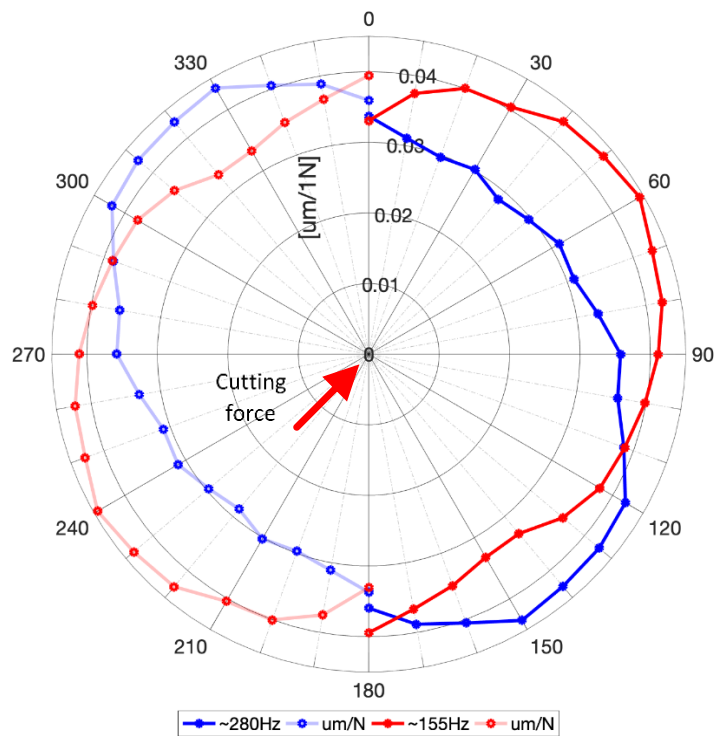


Fig. 9. Spindle dynamic compliance – polar chart

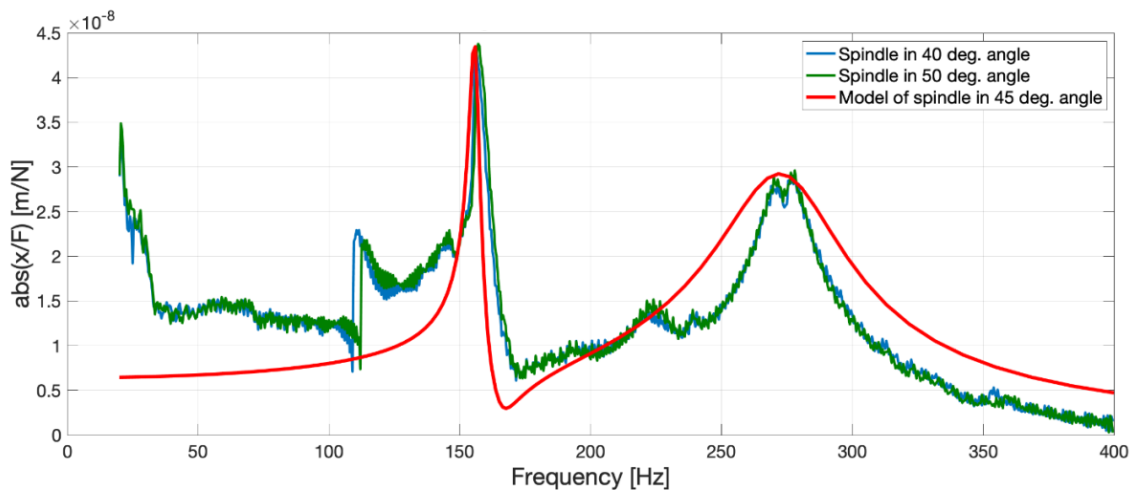


Fig. 10. 45 deg. directional spindle FRF

Spindle mathematical model is based on single mass on two springs, allowing movement only in 2D space area. The compliance of both perpendicular springs is based on the measured Transfer function and damping ratio of 5% is used. The transfer function describing this system can be derived based on Fig. 10 Motion equation of the system described above is written as equation (2).

$$M\ddot{x} + B\dot{x} + Kx = f \tag{2}$$

Where:

$$\ddot{x} = \begin{bmatrix} \ddot{y} \\ \ddot{x} \end{bmatrix} \quad \dot{x} = \begin{bmatrix} \dot{y} \\ \dot{x} \end{bmatrix} \quad x = \begin{bmatrix} y \\ x \end{bmatrix} \quad f = \begin{bmatrix} F_c \cdot \cos \beta \\ F_c \cdot \sin \beta \end{bmatrix} \quad (3)$$

For F_c as the cutting force and β as the cutting force angle (see Fig. 2 and Fig. 11).

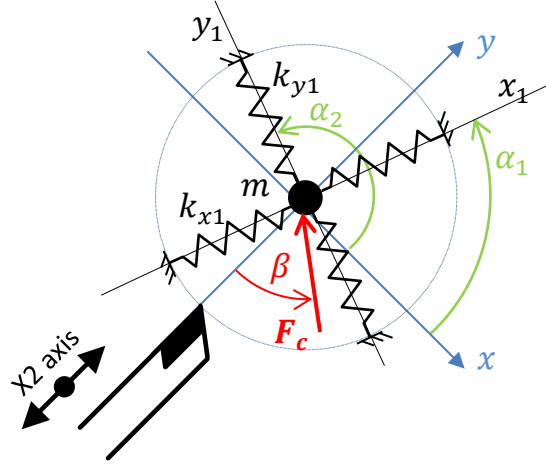


Fig. 11. Spindle model

Mass matrix **M**

$$\begin{bmatrix} m & 0 \\ 0 & m \end{bmatrix} \quad (4)$$

For m as the spindle mass.

Stiffness matrix **K**

$$\begin{bmatrix} k_{y1} \cdot \cos^2 \alpha_1 + k_{x1} \cdot \cos^2 \alpha_2 & k_{y1} \cdot \sin \alpha_1 \cdot \cos \alpha_1 + k_{x1} \cdot \sin \alpha_2 \cdot \cos \alpha_2 \\ k_{y1} \cdot \cos \alpha_1 \cdot \sin \alpha_1 + k_{x1} \cdot \cos \alpha_2 \cdot \sin \alpha_2 & k_{y1} \cdot \sin^2 \alpha_1 + k_{x1} \cdot \sin^2 \alpha_2 \end{bmatrix} \quad (5)$$

For the k_{y1} and k_{x1} as the perpendicular spring stiffness (see Fig. 11), α_1 and α_2 as the angles with the tool orthogonal system.

Damping matrix **B**

$$\begin{bmatrix} b_{y1} \cdot \cos^2 \alpha_1 + b_{x1} \cdot \cos^2 \alpha_2 & b_{y1} \cdot \sin \alpha_1 \cdot \cos \alpha_1 + b_{x1} \cdot \sin \alpha_2 \cdot \cos \alpha_2 \\ b_{y1} \cdot \cos \alpha_1 \cdot \sin \alpha_1 + b_{x1} \cdot \cos \alpha_2 \cdot \sin \alpha_2 & b_{y1} \cdot \sin^2 \alpha_1 + b_{x1} \cdot \sin^2 \alpha_2 \end{bmatrix} \quad (6)$$

For the b_{y1} and b_{x1} as the computed damping in perpendicular direction according to the spring orientation.

System transfer function is (Laplace transformation is used):

$$G(\text{spindle}) = \frac{x}{F_c} = \frac{1}{(Ms^2 + Bs + K)} \quad (7)$$

Matrix form with **G**-matrix

$$\begin{bmatrix} y \\ x \end{bmatrix} = \begin{bmatrix} G_{11} & G_{12} \\ G_{21} & G_{22} \end{bmatrix} \cdot \begin{bmatrix} F_C \cdot \cos \beta \\ F_C \cdot \sin \beta \end{bmatrix} \quad (8)$$

Where

$$G_{12} = G_{21} \quad (9)$$

Possible transfer functions for each direction based on acting force:

$$G_y(\text{spindle}) = \frac{y}{F_C} = G_{11} \cdot \cos \beta + G_{12} \cdot \sin \beta \quad (10)$$

$$G_x(\text{spindle}) = \frac{x}{F_C} = G_{21} \cdot \cos \beta + G_{22} \cdot \sin \beta \quad (11)$$

2.2. COUPLED MODEL AND FORCE DISTRIBUTION

Measured and identified transfer functions and composed models shown in Chapter 2.1 allows composing complete simulation model shown in Fig. 12 reflecting two parts verified in the experimental section. The black and blue line shows the dynamic compliance, hence the transfer function $G_y(\text{spindle})$ of the spindle mechanics described by the equation (10).

Feed drive part of the simulation model is based on the evaluation at the beginning of chapter 0 is represented by the black and red line. Used transfer function is composed of the whole regulation with the current regulation modelled by the low pass filter. PI regulation of velocity loop is used and the P regulation of position loop. The whole translation axis system is composed as 2 mass approximation with rotary elements included. Transfer function $G_y(\text{drive})$ between requested tool-tip position in the y -direction (according to Fig. 2) y_y and cutting force F_{cy} also in y -direction is assumed to be:

$$G_y(\text{drive}) = \frac{y_y}{F_{cy}} \quad (12)$$

The $G_y(\text{drive})$ transfer function includes the feed drive regulation and the mechanic structure of the $X2$ axis as shown in Fig. 12 The full system transfer function G_y in the milling axis $X2$ direction can be then proceeded as a sum of equation (10) and (12) as following equation (13). This one is used for the stability limits investigation. The full system includes

$$G_y(s) = G_y(\text{spindle}) + G_y(\text{drive}) \quad (13)$$

regenerative chatter vibration obtained from the previous workpiece revolution at the $e^{-\tau s}$ block, for the Simulink capsulation stability this time delay is modeled by the Padé approximant of second order. The cutting force F_C , computed as shown in (14), is in the model assumed to be in the $\beta = 70$ deg. angle from the plane parallel to the tool-tip.

$$F_C = -C_0 \cdot b \cdot y \tag{14}$$

The cutting force F_C is than projected to the axis X2 moving direction. Please note that the axis X2 direction is the y -direction in the simulation models, it is the direction of the translation movement of the tool. The equation (13) is also the crucial transfer function for the stability limits comparison. Adjusting the Laplace variable in the function where $s = j\omega$, the limit chip thickness b can be determined as:

$$b_{lim} = \frac{1}{2 \cdot C_0 \cdot |Re_{neg}G_y(j\omega)|} \tag{15}$$

Where the C_0 is the specific cutting resistance and $Re_{neg}G_y(j\omega)$ is the minimum of real part of the $G_y(s)$ transfer function.

The whole article uses the following numerical values for the examined system. The ABCD model of feed drive (in Fig. 3): $I_{motor} = 0.09 \text{ kg} \cdot \text{m}^2$, $I_{1pulley} = 0.00124651 \text{ kg} \cdot \text{m}^2$, $I_{2pulley} = 0.002241281 \text{ kg} \cdot \text{m}^2$, belt stiffness $k_{belt} = 773140 \text{ m} \cdot \text{N/m}$, pulley spacing $a = 0.376 \text{ m}$, ball-screw diameter $d = 50 \text{ mm}$ and pitch $h = 15 \text{ mm}$ feed drive motor constant $K_M = 1.43 \text{ Nm} \cdot \text{A}$, balls-crew nut stiffness $k_M = 279.5 \cdot 10^6 \text{ N m}^{-1}$, moving mass $m_T = 228.45 \text{ kg}$.

Used model of the lathe spindle is in configuration with the following parameters: $m = 60 \text{ kg}$, $k_{x1} = 177.8 \cdot 10^6 \text{ N} \cdot \text{m}^{-1}$, $k_{y1} = 57.6 \cdot 10^6 \text{ N} \cdot \text{m}^{-1}$, $\alpha_1 = -15^\circ$, $\alpha_2 = 75^\circ$. For the cutting simulation the specific cutting resistance $C_0 = 2.5 \cdot 10^9 \text{ N} \cdot \text{m}^{-2}$.

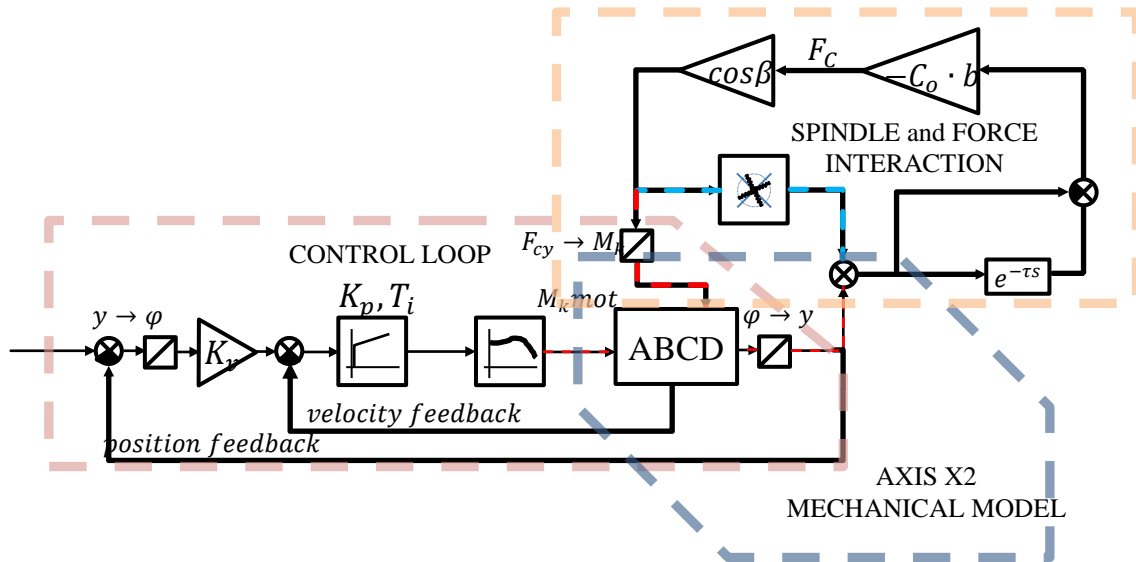


Fig. 12. Evaluation full system model

3. PROCESS STABILITY

For the further stability experiments, the series of parameters is chosen to demonstrate the shift in stability performance of the entire system. The selected parameters are shown in Table 1.

Table 1. Parameters selection

	K_p [(m/min)/mm]	T_n [ms]	K_p [Nms/rad]
1 ST SET	7	10	3
2 ND SET	2	10	1
3 RD SET	1	10	0.5
4 TH SET	5	10	2

The system behaviour is demonstrated on the amplitude characteristic shown in Fig. 13, along with the amplitude characteristics, the Real part of the $G_y(s)$ transfer function is plotted with the axis in 30 mm from its higher stroke. Based on the equation (15) the critical depth of cut is calculated for each set of parameters in Table 2. The difference can be seen in comparison of the 1st set of parameters, usually used for usual cutting and for the 3rd set of parameters, where the critical depth of cut decreases significantly.

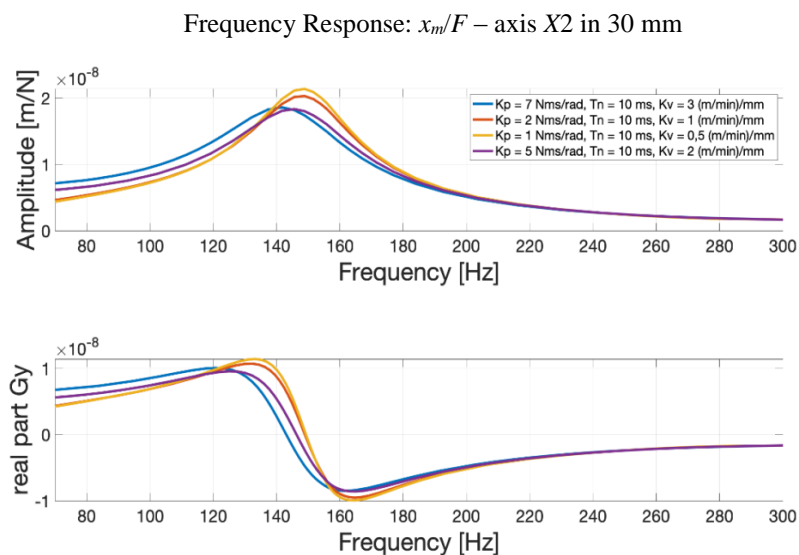
Fig. 13. System transfer function x/F

Table 2. Critical depth of cut

	Depth of cut [mm]	Depth of cut ratio [%]
1 ST SET	23.6	100
2 ND SET	21.1	89.4
3 RD SET	18.1	76.7
4 TH SET	23.3	98.7

4. FEED DRIVE ANALYSIS

The mathematical model of the feed drive of the X2 axis of the middle size lathe as described above have been subjected to the velocity step response analysis in Fig. 14. It can be clearly seen that all of the sets of feed drive parameters are giving sufficient response. Neither set of parameters brings a highly oscillating response, so all are usable for

the manufacturing purposes. The Second verification of the selected feed drive constants is done by the study of position ramp response shown in Fig. 15 There is clearly seen that the combination of higher K_p and K_v reaches the requested position rapidly, but all of the investigated parameters are again usable for the machining as neither combination exceed the requested position. The first set of the parameters with $K_v = 3$ (m/min)/mm, $K_p = 7$ Nms/rad, $T_n = 10$ ms is clearly the best set-up for the actual mechanical configuration. Due to the rapid velocity settlement as well. The velocity step response also shows slight oscillation around the estimated value, so it can be considered that additional K_p and K_v rise can lead to an unstable system.

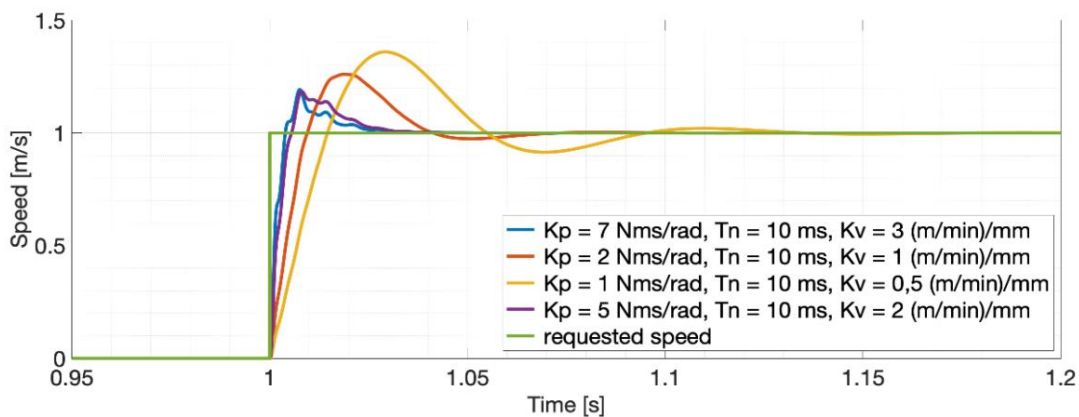


Fig. 14. Velocity step response

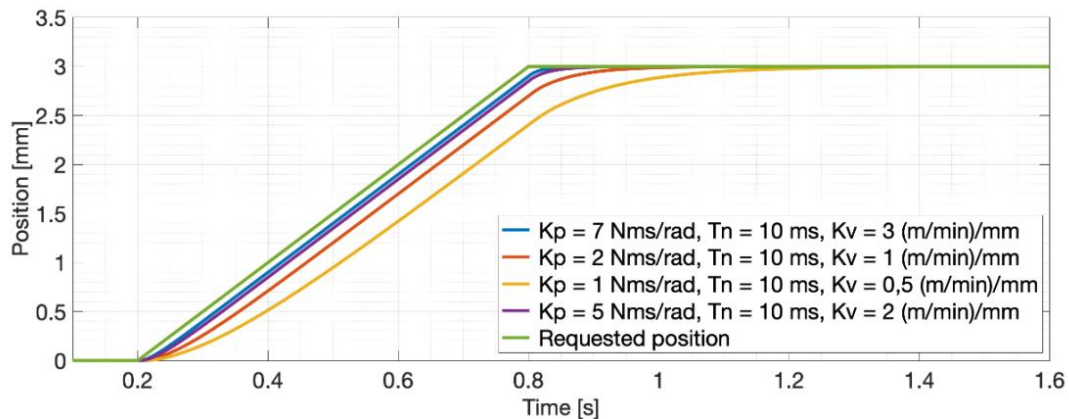


Fig. 15. Position ramp response

5. CONCLUSION

In this paper, the middle size lathe was taken under inspection. More specifically the X2 axis and its influence on process stability. The X2 axis investigation takes into account the axis mechanic structure and dynamic parameters of feed drive control. Moreover, the whole stability model was complemented by the lathe spindle mechanics with its dynamic

compliance. The complete MATLAB – Simulink model was developed based on the conclusion provided by measurement.

Spindle lathe was analysed by the vibro-diagnostic equipment using the force exciter. The 2D plane dynamic compliance was recorded and based on the measured transfer function, the mathematical model was created.

X2 axis feed drive was modelled based on the parameters copied from the Sinumerik controlling system and on the transfer function extracted from the control system as well. Final feed drive model was created as the state-space model, which is implemented into the current, velocity and position control loop

The Resulting mathematical model for the machining stability analysis includes the ball screw drive dynamics, spindle dynamics and force interaction between the tool and spindle. Using the model, calculation of the critical depth of cut has been performed.

The results prove that the parameter setting of the ball screw drive controller can shift the limit of stable depth of cut by up to approx. 25%. Research of the effect of feed drive controller setting considering the whole machine tool structure is a perspective of the continuing work.

ACKNOWLEDGEMENTS

This work was supported by the Grant Agency of the Czech Technical University in Prague, Reg. No. OHK2-007/19.

REFERENCE

- [1] QUINTANA G., CIURANA J., 2011, *Chatter in machining processes: A review*, International Journal of Machine Tools and Manufacture, 51/5, 363–376.
- [2] TAYLOR F.W., 1907, *On the art of cutting metals*, New York, American Society of Mechanical Engineers, 2888763.
- [3] TLUSTY J., POLACEK M., 1963, *The stability of machine tools against self-excited vibrations in machining*, Proceedings of the ASME International Research in Production Engineering, 465–474.
- [4] TOBIAS S.A., FISHWICK W., 1958, *A theory of Regenerative chatter*, The Engineer-London.
- [5] MERRITT H.E., 1965, *Theory of Self-Excited Machine-Tool Chatter: Contribution to Machine-Tool Chatter Research*, Journal of Engineering for Industry, 87, 447–454.
- [6] ALTINTAS Y., BUDAK E., 1995, *Analytical Prediction of Stability Lobes in Milling*, CIRP Annals – Manufacturing Technology, 44/1, 357–362.
- [7] STONE B., 2014, *Chatter and Machine Tools*, Springer International Publishing, 978-3-319-05235-9.
- [8] KOLAR P., et al. 2012, *An integrated approach to the development of machine tool structural parts*, MM Science Journal, 9th International Conference on Machine Tools, Automation, Technology and Robotics MATAR, 1–7.
- [9] KOLAR P., et al. 2013, *Modern Methods for efficient Machine Tool Design*, 10th International Conference on High Speed Machining, Darmstadt: Abele, Metternich, 26–27.
- [10] MÖHRING H.-Ch., et al., 2017, *Intelligent Hybrid Material Slide Component for Machine Tools*, Journal of Machine Engineering, 17/1, 31–45.
- [11] ITO Y., 2013, *Position Paper – Fundamental Issues in Self-excited Chatter in Turning*, Journal of Machine Engineering, 13/3, 7–25.
- [12] COWLEY A., BOYLE A., 1970, *Active Dampers for Machine Tools*, CIRP Anals, 18/1, 213–222.
- [13] BLEICHER F., SCHÖRGHOFER P., HABERSOHN C., 2018, *In-process control with a sensory tool holde to avoid chatter*, Journal of Machine Engineering, 18/3, 16–27.
- [14] MUNOA J., et al., 2015, *Active Suppression of Structural Chatter vibrations Using Machine Drives and Accelerometers*, Annals of the CIRP, 64/1, 385–388.

- [15] NOVOTNY L., et al., 2018, *Damping in machine tool structure*, Proceedings of 14th International Conference on High Speed Machining: Productivity, Quality and Digitalization, San Sebastian: Uriate, Munoa, 17–18 April.
- [16] BILBAO-GUILLERNA A., BARRIOS A., MANCISIDOR I., et al., 2010, *Control laws for chatter suppression in milling using an inertial actuator*, Proceedings of ISMA, International Conference on Noise and Vibration Engineering, Sep., 1–12.
- [17] LEHOTZKY D., TURI J., INSPERGER T., 2014, *Stabilizability diagram for turning processes subjected to digital PD control: A review*, International Journal of Dynamics and Control, 2195-268X, 2/1, 46–54.
- [18] BEUDAERT X., et al., 2016, *Analysis of the feed drives control parameters on structural chatter vibrations*, XIII International Conference on High Speed Machining (HSM2016), LEM3, Oct 2016, Metz, France, hal-01484796.
- [19] SLAVIK J., STEJSKAL V., ZEMAN V., 1997, *Zaklady dynamiky stroju*, Praha, CVUT, 80-01-01622-6.